

# Injectable Chemically Crosslinked Hydrogel for the Controlled Release of Bevacizumab in Vitreous: A 6-Month In Vivo Study

Yu Yu<sup>1</sup>, Laurence Chi Ming Lau<sup>2</sup>, Amy Cheuk-yin Lo<sup>2</sup>, and Ying Chau<sup>1,3</sup>

<sup>1</sup> Division of Biomedical Engineering, The Hong Kong University of Science and Technology, Clear Water Bay, Kowloon Hong Kong, China

<sup>2</sup> Department of Ophthalmology, The University of Hong Kong, Pok Fu Lam, Hong Kong, China

<sup>3</sup> Department of Chemical and Biomolecular Engineering, The Hong Kong University of Science and Technology, Clear Water Bay, Kowloon, Hong Kong, China

**Correspondence:** Ying Chau, Room 4353, Academic Building, The Hong Kong University of Science and Technology, Clear Water Bay, Kowloon, Hong Kong, China; e-mail: ying.chau@ust.hk

**Received:** 28 June 2014

**Accepted:** 3 November 2014

**Published:** 10 March 2015

**Keywords:** hydrogel; Bevacizumab; controlled release; avastin; ocular delivery

**Citation:** Yu Y, Lau LCM, Lo AC-Y, Chau Y. Injectable chemically cross-linked hydrogel for the controlled release of bevacizumab in vitreous: a 6-month in vivo study. *Trans Vis Sci Tech.* 2015;4(2):5, <http://tvstjournal.org/doi/full/10.1167/tvst.4.2.5>, doi:10.1167/tvst.4.2.5

**Purpose:** To evaluate the biocompatibility and 6-month in vivo release of bevacizumab from a hyaluronic acid/dextran-based in situ hydrogel after intravitreal injection in rabbit eye.

**Methods:** The in situ hydrogel was formed by the catalyst-free chemical crosslinking between vinylsulfone functionalized hyaluronic acid (HA-VS) and thiolated dextran (Dex-SH) at physiological condition. The pH 7.4 buffered mixture containing HA-VS, Dex-SH, and bevacizumab were injected into the vitreous of rabbit eyes by a 30-G needle. The biocompatibility was evaluated by intraocular pressure measurement, binocular indirect ophthalmoscope (BIO), full-field electroretinogram (ERG), and histology. The concentrations of both total and active bevacizumab in rabbit vitreous were determined by enzyme-linked immunosorbent assay. The concentration of bevacizumab in rabbit vitreous after bolus injection was simulated by one-compartment first order elimination model.

**Results:** A transparent gel was seen in the vitreous after injection. BIO images, ERG, and histology showed that the gel does not induce hemorrhage, retinal detachment, inflammation, or other gross pathological changes in rabbit eyes after injection. While the bolus intravitreal injected bevacizumab follows the first order elimination kinetics in rabbit eye, the in situ gel formation was able to prolong the retention of bevacizumab in rabbit eye at therapeutic relevant concentration for at least 6 months. The concentration of bevacizumab 6 months after injection was about  $10^7$  times higher than bolus injection.

**Conclusions:** The new in situ hydrogel formulation of bevacizumab was biocompatible and able to prolong the retention of drug in rabbit eyes in vivo at therapeutic relevant concentration for at least 6 months.

**Translational Relevance:** Although proven to be effective, monthly intravitreal injection of bevacizumab or other protein drugs may cause various complications. Extending the residence time of protein therapeutics in the eye can reduce the injection frequency, its associated complications, and treatment cost, which will be beneficial to both the patients and doctors. In this study, we showed that the in situ hydrogel-based controlled release system is a feasible option to tackle this problem.

## Introduction

In the last decade, the application of anti-vascular endothelium growth factor (VEGF) antibodies as the treatment for ocular neovascularization diseases, such as age-related macular degeneration (AMD) and

diabetic retinopathy (DR), has gained huge acclaim because of their superior performance over small molecular drug and the ability to restore vision for patients.<sup>1</sup> Examples of these drugs include Avastin (Roche Ltd., Basel, Switzerland), Lucentis (Roche Ltd., Basel, Switzerland), and Eylea (Regeneron Pharmaceuticals, Inc., New York, NY). However,

because of the high clearance rate of drugs in the vitreous and the chronic nature of these diseases, monthly intravitreal injection is required for a satisfactory treatment,<sup>2,3</sup> which significantly increases the risk of complications.<sup>4</sup> The psychological and economic burdens further reduce the patient compliance.<sup>2</sup>

A potential solution to this problem is to develop an injectable controlled release depot to extend the residence time of drugs in the eye so that injection frequency can be reduced. An ideal delivery system should satisfy the following criteria:

1. It should be able to control the release of protein in its active form and maintain above therapeutic concentration for at least 3 months.
2. It should be biocompatible to the eye.
3. It should be injectable and eventually degradable in the eye.
4. The disturbance to vision should be minimized.

Chemically crosslinked polymer-polymer in situ gel is one of the platforms that can potentially fulfill these criteria. This type of in situ hydrogel is prepared by mixing two or more polymer components that can form chemical crosslinks at physiological conditions. The mixture is an injectable liquid but solidifies quickly by chemical crosslinking after injection. The hydrophilic nature of this system avoids the potential destruction of higher-level structures of labile biomacromolecules, which is an advantage over the implant system composed of hydrophobic polymer. The adjustable network structure can be used to control the drug release at a desirable rate.<sup>5</sup> Chemical crosslinking from polymer-polymer reaction also allows the choice of a wide range of biocompatible and degradable polymer. In recent years, this type of hydrogel has been approved for clinical use in various applications including cardiovascular diseases and lung diseases.<sup>6</sup>

Previously, we have developed a simple model to predict hydrogel properties from the precursor polymer properties.<sup>5</sup> Using this model as a guideline, we have designed a hyaluronic acid (HA)/dextran-based in situ gel system for the controlled release of bevacizumab.<sup>5</sup> This system is composed of vinyl-sulfone functionalized HA (HA-VS) and thiolated dextran (Dex-SH). HA was chosen as one of the main components because of its degradability in the eye.<sup>7-9</sup> Both HA and dextran have been used extensively in ophthalmological applications and have excellent safety records.<sup>10</sup> By simply mixing the two polymers and the therapeutic protein, a hydrogel-based controlled release depot can be formed without using any

initiator or generating any by-product. By controlling the concentration and degree of modification (DM) of these two polymers, we were able to construct a transparent hydrogel to release bevacizumab for at least 3 months.<sup>5</sup>

In this study, the cyto and in vivo biocompatibility of this gel, as well as the in vivo release of gel-formulated bevacizumab after intravitreal injection to rabbits, were evaluated.

## Methods

### Materials

All chemicals for polymer modification were purchased from Sigma (St. Louis, MO) unless specified. HA of 29 kDa was purchased from Bloomage Freda Biopharm Co., Ltd. (Jinan, China). Avastin was purchased from Roche Ltd. A sterile 0.22- $\mu$ m syringe filter (Millex GP) was purchased from Merck Millipore (Billerica, MA). ARPE-19 cell was obtained from ATCC (Manassas, VA). Dulbecco's modified Eagle medium (DMEM) nutrient mixture F12 (DMEM-F12 1:1), fetal bovine serum (FBS), and penicillin/streptomycin were purchased from Gibco (Invitrogen, Gaithersburg, MD). Live/Dead assay reagents were purchased from Life Technologies (Norwalk, CT). Mydriacyl, Alcaine, Maxitrol and artificial tear (Tear Naturale II) were purchased from Alcon Laboratories Ltd. (Camberley, Surrey, UK). Xylazine, ketamine, and pentobarbital were purchased from Alfasan International B.V. (Woerden, Holland). Povidone-iodine (Betadine) was purchased from Purdue Products L.P. (Stamford, CT). AffiniPure Rabbit Anti-Human IgG (H+L) was purchased from Jackson ImmunoResearch Laboratories, Inc. (West Grove, PA). Protein Detector HRP Microwell Kit (anti-human) was purchased from KPL, Inc. (Gaithersburg, MD). VEGF<sub>165</sub> was purchased from Sino Biological, Inc. (Beijing, China).

### Preparing Chemically Crosslinkable Polymers

HA-VS and Dex-SH were made according to our previous publications.<sup>5,11</sup> Briefly, HA-VS of 20% DM was made by reacting with 1.25 $\times$  (DVS:OH) molar excess of DVS with HA at 0.1 M NaOH for 2 minutes 45 seconds and stopped by neutralizing with HCl. After purification with tangential flow filtration (TFF, mPES MidiKros TFF Filter, NMWL = 3 kDa, D02-E003-05-N, Spectrum Laboratory, Inc., CA), the polymers were adjusted to pH 5.2, sterilized by filtering through a 0.22- $\mu$ m syringe filter (Millex GP, Merck Millipore Ltd.),

and freeze dried. For the preparation of Dex-SH, dextran was first converted to Dex-VS by reacting with 1.25× (DVS:OH) molar excess of DVS in 0.02 M NaOH for 2 minutes 20 seconds. Dex-SH was made by reacting Dex-VS with excess amount of dithiothreitol (DTT) in N<sub>2</sub>. The polymers were purified by TFF, adjusted to pH 5.2, sterilized by filtering through a 0.22- $\mu$ m filter, and freeze dried. The characterization of polymers was done according to our previous publications by using <sup>1</sup>H Nuclear Magnetic Resonance (<sup>1</sup>HNMR) and Ellman's assay.<sup>5,11</sup>

### Cell Culture and Cytocompatibility of Hydrogel

ARPE-19 cells were maintained according to published protocols.<sup>12</sup> The cytocompatibility of hydrogel incubation and the in situ gelation process were examined by the Live/Dead assay (Life Technologies). ARPE-19 cells were seeded in a 96-well plate at a density of about  $6 \times 10^4$  cell/mL in 100  $\mu$ L culture medium. The cells were grown for 24 hours before adding hydrogels or polymer. For the hydrogel incubation study, HA-VS and Dex-SH were dissolved in phosphate-buffered saline (PBS) separately and mixed to form hydrogels of about 5  $\mu$ L in size by dropping the polymer mixture on a Parafilm (Bemis Company, Inc., Neenah, WI). The gels were first equilibrated in culture medium, and then placed in the cell-seeded wells. Each piece of gel sank to the bottom and covered about two-thirds of the area of one well. For examining the in situ gelation process, the polymers were first dissolved in PBS separately and mixed. Before the polymer mixture becomes solidified (about 30 seconds), a 5- $\mu$ L mixture was added on the cell-seeded well. The polymer sunk and covered the cells at the bottom and solidified shortly. For both studies, the cells were incubated for another 24 hours in the presence of gels, then Calcein AM and Ethidium homodimer-1 were added to the well without washing to a final concentration of 2  $\mu$ M and 4  $\mu$ M. After 30 minutes incubation at 37°C, the cells were imaged by a fluorescent microscope (Eclipse TE2000-U; Nikon, Tokyo, Japan) at 400× according to the Live/Dead assay (Life Technologies) manual instruction. For each well, five random locations were selected and imaged. Four repeats were done for each formulation. For the live control experiment, no gel or polymer was added to the cells. For dead control experiment, no gel or polymer was added to the cells, and water was used to replace culture medium during incubation.

The percentage of live cells was quantified by

counting the number of live cells over the total amount of cells (live + dead cells) from each image.

### Animals

Female New Zealand White rabbits (NZW, 5.5 to 7 months old at the starting point of the experiments) were used in this study. The use of rabbits followed the animal study guidelines of the Association for Research in Vision and Ophthalmology (ARVO) and was approved by the Committee on the Use of Live Animals in Teaching and Research (CULATR 2683–12) of The University of Hong Kong, The Animal Ethics Committee of The Hong Kong University of Science and Technology, and the Department of Health of Hong Kong.

The left eyes of rabbits received intravitreal injection, and the right eyes were left unoperated. Before all treatments, the rabbits were anesthetized with intramuscular injection (0.8 mL/kg body weight) of a mixture of 2% xylazine/10% ketamine at a ratio of 1:1. The corneas were topically anesthetized with Alcaine (Alcon Laboratories Ltd.). The pupils were dilated with topical application of Mydracyl (Alcon Laboratories Ltd.).

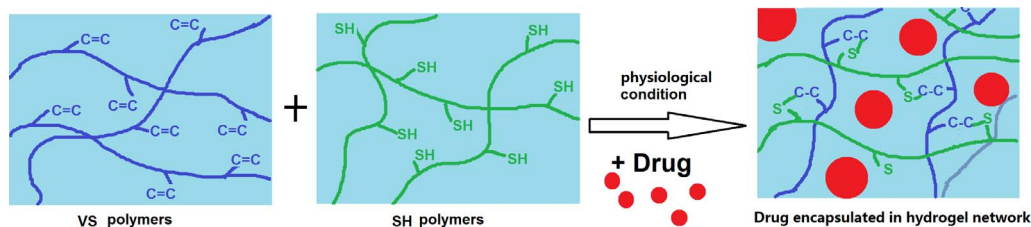
### Intravitreal Injection of Gel and Gel-Formulated Bevacizumab in Rabbit Eye

Before injection, the ocular surface was sterilized by application of 3% Betadine (Purdue Products L.P.) and washed with saline. HA-VS and Dex-SH were dissolved in sterilized PBS separately. After complete dissolution, the polymers were placed on ice. Afterwards, the polymers were mixed, loaded into a precooled syringe, and injected to the left eye of rabbit via a 30-gauge needle at the pars plana 3 mm behind the limbus at the superior temporal region. The volume for each injection was about 40  $\mu$ L.

For gels encapsulating bevacizumab, the Avastin (Roche Ltd.) solution was first adjusted to pH 7.4 by drop wise addition of 1 M NaOH. This solution was used to dissolve the HA-VS. To minimize the potential reaction between bevacizumab and the VS group,<sup>5</sup> the dissolution time was limited to 10 minutes. Dex-SH was dissolved in PBS. The two polymers were cooled on ice. The mixing and injection procedure was identical to the gel injection.

After injection, Maxitrol (Alcon Laboratories Ltd.) was applied to prevent infection and suppress inflammation.

A schematic showing the crosslinking and encapsulation of the drug is shown in Scheme 1.



**Scheme 1.** Schematic showing the gelation reaction and the spontaneous encapsulation of drug in the hydrogel network.

## Examination Using Binocular Indirect Ophthalmoscope (BIO)

The hydrogel and the fundus of rabbit eyes *in vivo* were checked and digitally recorded regularly for all rabbits by digital BIO (Vantage Plus LED version, Keeler Ltd., Windsor, UK) with 20 diopter BIO lens (Volk Optical, Inc., Mentor, OH). The corneas were hydrated by artificial tear before imaging. For each eye, the center (optic disc), superior temporal (injection site), superior nasal, and inferior quadrant were examined.

## Intraocular Pressure (IOP) Measurement

The IOP was measured on anesthetized rabbits by a tonometer (Tono-Pen XL, Mentor, MedWOW, Nicosia, Cyprus) according to the manufacturer's manual instruction. The values were measured before injection, after injection, and during eye examinations for all animals.

## Assessment of Retinal Function by Electroretinogram (ERG)

Full-field ERG (PS33-PLUS; Natus Neurology, Inc., Warwick, RI) was measured before injection, and at 1, 4, and 12 weeks after injections. For each time point, at least five rabbits were used.

Rabbits were anesthetized with pupils dilated as earlier described. ERG signals were recorded by a unipolar corneal electrode (ERG-jet; Fabrial, La Chaux-de-Fonds, Switzerland), a reference electrode inserted into the eyelid, and a ground electrode inserted beneath ear skin. The flash intensity was set at 5.5 lumen sec/ft<sup>2</sup>, and the duration was 10  $\mu$ s. The signals were amplified by an amplifier (CP511 A.C. amplifier; Natus Neurology, Inc.) at 20,000 gain and filtered between 1 and 300 Hz. A single flash was delivered every 15 seconds for the light-adapted ERG and every 35 seconds for the dark-adapted ERG. Light-adapted ERG responses were recorded under 20 cd/m<sup>2</sup> background luminance. Rabbits were adapted in dark environment for 30 minutes prior

to the dark-adapted ERG. The A-wave amplitude was measured from the baseline to the trough, and the b-wave amplitude from the trough to the peak. The posttreatment ERG amplitudes were normalized as the fold change relative to pretreatments.

## Assessment of Retinal Structure by Histological Analysis

For each experimental group, at least five rabbits were used. Rabbits were euthanized after reaching their experimental end points by the rapid intravenous injection of pentobarbital at marginal ear veins. The peripheral oxygen and heart rate were monitored with a pulse oximeter (Avant 9600 Tabletop Pulse Oximeter; Nonin Medical, Inc., Plymouth, MN). The left eyes were enucleated and fixed in 4% paraformaldehyde in PBS overnight, then dehydrated in graded series of alcohol and chloroform, followed by paraffin embedding. Sections of 6- $\mu$ m thickness were serially cut with a microtome (Microm HM 315R; Heidelberg Engineering, Heidelberg, Germany) along the temporal-nasal equator, and stained with hematoxylin and eosin (H&E). The retinal area at the central-temporal visual streak was analyzed and compared among various experimental groups. Slides were examined under a light microscope of 400 $\times$  magnification (Eclipse 80i; Nikon Instruments, Inc., Tokyo, Japan). Pictures were taken with a digital camera (SPOT RT3; Diagnostic Instruments, Inc., Sterling Heights, MI). Thickness of the outer nuclear layer (ONL) and inner nuclear layer (INL) were measured.

## Detection of Bevacizumab in the Vitreous Using Enzyme-Linked Immunosorbent Assay (ELISA)

The amount of bevacizumab in the rabbit vitreous was measured by two Sandwich ELISA methods. The first method used polyclonal rabbit anti-human IgG as coating for the measurement of total amount of bevacizumab,<sup>13</sup> and the second method used VEGF as coating to measure the active bevacizumab.<sup>14,15</sup> The

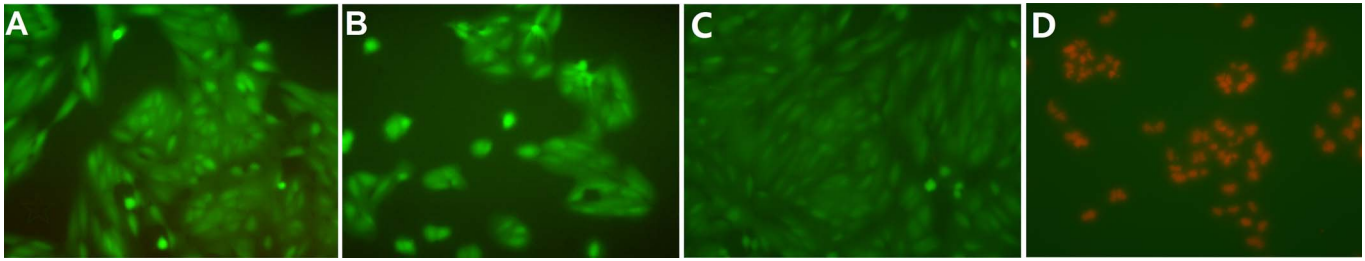


**Figure 1.** Representative images showing the Live/Dead (Life Technologies) staining of ARPE-19 cells. (A) Incubated with well-form hydrogel for 1 day and (B) exposed to in situ gel formation and incubated for 1 day. (C) Live control. (D) Death control.

ELISA protocol was developed according to KPL's guideline. Briefly, 100  $\mu\text{L}$  rabbit anti-human IgG or VEGF of concentration 0.6 or 0.3  $\mu\text{g}/\text{mL}$  were coated on the plate for overnight at 4°C. After washing and blocking, 90- $\mu\text{L}$  series diluted samples were added to the wells and incubated for 2 hours in room temperature. After washing, 100  $\mu\text{L}$  secondary antibody of 0.25  $\mu\text{g}/\text{mL}$  were added to the well for 1 hour in 4°C or at room temperature for total and active bevacizumab measurement. After washing, 100  $\mu\text{L}$  substrate was added, and the reaction was stopped by adding 1% sodium dodecyl sulfate (SDS) after color developed, usually about 3 minutes for total bevacizumab and 6 minutes for active bevacizumab measurement.

The bevacizumab concentration in the rabbit eyes were examined 1 week, 2 weeks, 1 month, 3 months, and 6 months post injection. For each time point, at least three animals were used. Originally, we planned to perform longitudinal studies by aspirating the vitreous from the same rabbits at different time points. However, when we performed this procedure at week 1, we observe hemorrhage at the insertion site in some rabbits. We therefore later on used different rabbits for different time points similar to published bevacizumab ocular pharmacokinetics procedures.<sup>13–15</sup> The rabbits of the 6-month group were the nonhemorrhaged rabbits after vitreous aspiration at week 1.

ELISA experiments were performed 1 day after harvesting the vitreous (stored at 4°C before testing). Bevacizumab standard ( $n = 3$ ) was tested along with vitreous samples during every test to reduce inter-experimental differences. Each vitreous sample was measured with both ELISA methods and repeated three times.

### Mathematical Simulation

The concentration of bevacizumab in the rabbit eye after bolus intravitreal injection was simulated based on the first order elimination model<sup>13–16</sup>:

$$\frac{dM}{dt} = -kM_i$$

Where  $k = \sqrt{2}/T_{1/2}$  and the half life  $T_{1/2}$  was taken as 5.5 averaging from published bevacizumab pharmacokinetics studies in rabbits.<sup>13–15</sup> Because the concentration of bevacizumab in the gel was 12.5  $\text{mg}/\text{mL}$  and the volume injected was about 40  $\mu\text{L}$ , an initial mass of 500  $\mu\text{g}$  was used in the simulation.

The concentration of bevacizumab in the rabbit eye after gel-formulated injection was simulated using one compartment pharmacokinetics model:

$$\frac{dM_a}{dt} = \frac{dM_r}{dt} - kM_a$$

Where  $M_a$  is the mass of bevacizumab in the vitreous, and  $M_r$  is the mass released from the hydrogel.  $dM_r/dt$  was determined from curve fitting using Excel (Microsoft, Redmond, WA) to the in vitro release profile (Supplementary Fig. S1). The concentration was calculated by assuming the volume of the rabbit vitreous is 1.5 mL.

The equations were solved using PolyMath (Polymath Software, Willimantic, CT).

### Statistics

Data were presented as mean  $\pm$  SD. Kruskal-Wallis test followed by Dunnett's multiple comparison test was performed for data analysis (GraphPad Prism 5.0; GraphPad Software, La Jolla, CA). A statistically significant difference was stated when  $P < 0.05$ .

## Results

### Cytocompatibility of Hydrogel

The cytocompatibility was tested using ARPE-19 cells. It was found that  $98.9 \pm 0.46\%$  and  $99.42 \pm 0.52\%$  of cells were alive (stained green) after exposure to the gelation process and the well-formed hydrogel, suggesting that the gel is cytocompatible. The results

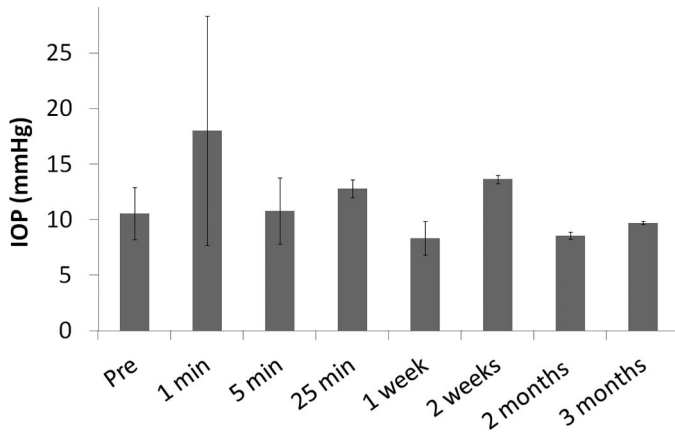


**Figure 2.** IOP at different time points after gel-formulated bevacizumab injection.

were consistent in all repeats. Representative images are shown in [Figure 1](#).

### IOP Measurement

We found that the IOP increased about two to three times after injection but returned to normal after about 5 minutes. [Figure 2](#) shows the IOP change in rabbit eyes receiving bevacizumab encapsulated gel ( $n \geq 3$ ) at different time points.

### Assessment of Retinal Morphology by BIO

After injection of blank gel or bevacizumab encapsulated gel, the overall morphology of the retina and blood vessels remained unchanged. The cornea and the lens remained clear during the examination period. No retinal detachment, edema, or inflammation was observed at all quadrants. [Figure 3](#) shows representative images of rabbit eyes after bevacizumab encapsulated hydrogel injection at different time points. Only images of the superior temporal region

(gel injection site) were shown as a representative of the other quadrants.

### Assessment of Retinal Function by ERG

The fold change in ERG value after gel injection at different time points was compared with PBS injection ([Fig. 4](#)). For the control group receiving PBS injection, ERG fluctuation was observed when measured at a different time. The range of fluctuation of ERG of gel injection eyes was similar to the control, indicating that the electrophysiology functions of photoreceptors and secondary neurons were not affected by the presence of gel in the vitreous body.

### Assessment of Retinal Structure by Histological Analysis

All layers of retina were normal without major changes ([Fig. 5](#)). No macrophage infiltration, edema, or swelling was found in eyes injected with gels or bevacizumab encapsulated gels. The cell density of INL and ONL of the treated eyes were similar to that of the control. The thickness of cell layers was also similar to the control group ([Fig. 6](#)).

### Bevacizumab Concentration in the Vitreous

The concentrations of the total and active bevacizumab in the vitreous were measured by ELISA. The result shows that the concentration in the vitreous was at therapeutically relevant concentration ( $\sim 50 \mu\text{g/mL}$ ) even 6 months after injection ([Fig. 7](#)). At the sixth month, the concentration was about  $10^7$  times higher in gel formulation than bolus injection of bevacizumab according to the simulation. The experimental measurements also correlate well with the simulation results for the intraocular concentration of bevacizumab after the injection of the gel formulation.

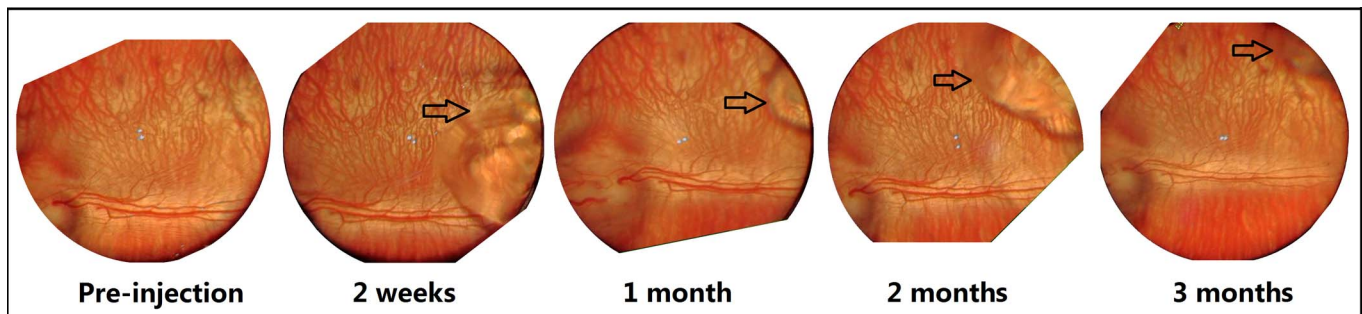


**Figure 3.** BIO images of a rabbit eye receiving bevacizumab encapsulated gel at different time points. Arrow indicates the boundary of hydrogel.

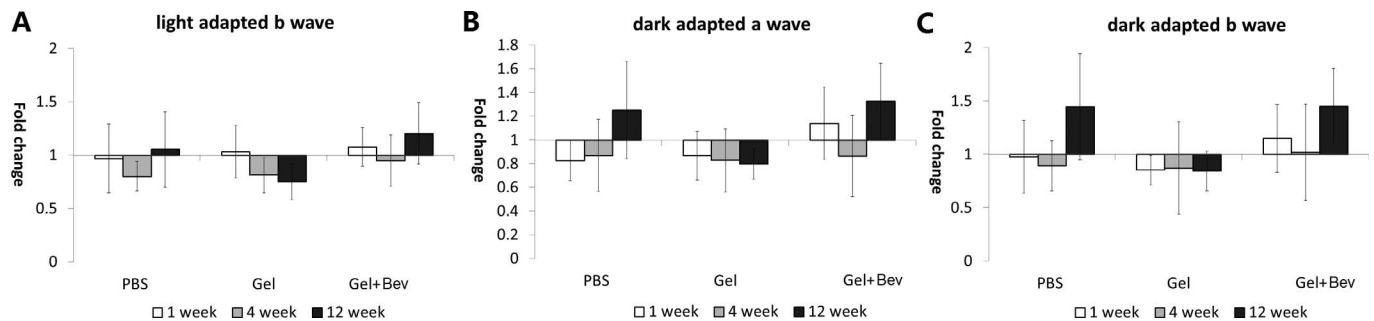


**Figure 4.** Fold change of full-field ERG in rabbits injected with PBS, hydrogel, or bevacizumab encapsulated gel. The level of fluctuation was similar between control group and the gel injection groups. The difference between the control group and gel injection groups at the same time points was not statistically significant either ( $P > 0.05$ ).

## Discussion

The quest to extend the residence of bevacizumab or other protein drugs in the eyes has triggered the exploration of various controlled release systems in the eye in the recent decade.<sup>17</sup> Among these approaches, in situ hydrogels have gained increasing attention in the recent 2 years because of the mild encapsulation condition and the hydrophilic nature of the network.<sup>18–23</sup> Different from our approach of using chemically crosslinked polymer-polymer in situ gel, a majority of other studies utilized physically crosslinked thermosensitive hydrogels as the controlled release vehicles. However, although promising in vitro protein release has been demonstrated by this approach,<sup>19,21</sup> the in vivo performance was not satisfactory and has only been demonstrated in one study.<sup>22</sup> Moreover, hydrophobic interaction between protein and the polymer may potentially affect the chemical or physical stability of the protein.<sup>24</sup> The nontransparent appearance of these gels may also hinder its application in the eye. A chemically crosslinked gel system for bevacizumab delivery in

the eye was recently published.<sup>25</sup> However, because the hydrogel was made by UV-induced polymerization of monomers, the injection site is limited to confined spaces like suprachoroidal space to prevent fast dissolution of the monomer. These spaces are still difficult to be accessed in the human eye clinically. The use of monomers, photoinitiator, and UV may also raise biocompatibility issues when applied in human.

Different from these approaches, we believed that chemically crosslinked polymer-polymer hydrogels may be a better approach for formulating intraocular protein release depot because it can potentially fulfill the criteria we proposed in the Introduction section.

We first examined the biocompatibility of the gel formulation used in this study. Using ARPE-19 cells, the gelation process and gel incubation were found to be compatible to ocular cells in vitro (Fig. 1). The cells exposed to in situ gelation were less spread out compared to gel incubation or control, this is because cells are known not to adhere to HA and dextran hydrogel.<sup>26,27</sup> However, cell death (red stain) was not

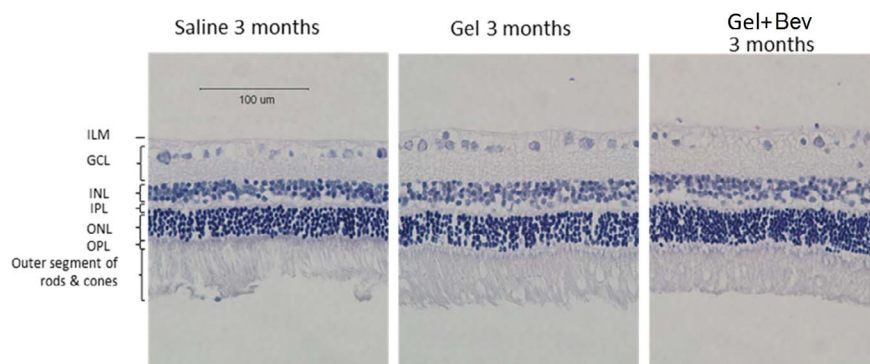


**Figure 5.** Histology of retinal H&E sections of rabbit eye receiving PBS control, hydrogel, or bevacizumab encapsulated hydrogel after 3 months.

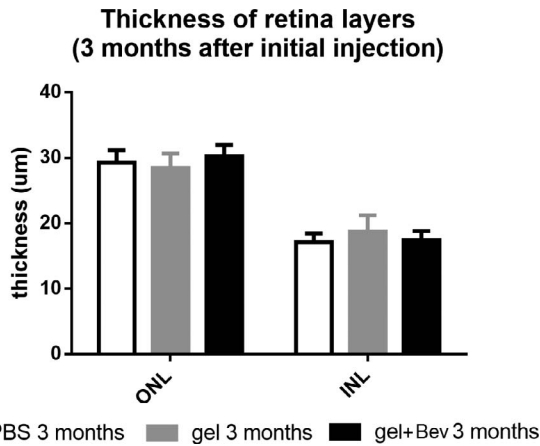


**Figure 6.** Thickness comparison of ONL and INL of rabbit retina with injection of PBS, gel, or bevacizumab encapsulated gel ( $P > 0.05$ ).

observed in the two experimental groups, indicating that the gel did not reduce cell viability.

The *in vivo* biocompatibility was examined by IOP measurements, BIO observations, ERG, and histology. For IOP measurements, we found that with the current volume of injection, the IOP increased twofold to threefold right after injection and returned to normal a few minutes later (Fig. 2), which was similar to saline injection (data not shown). The trend is consistent with other reports on intravitreal *in situ* gel injection.<sup>22</sup> The value of IOP elevation was not as high as other reports, because we injected 40  $\mu$ L instead of 50  $\mu$ L gel (as used by other authors) intentionally to minimize IOP elevation and allow faster recovery. Conditions associated with IOP elevation including cataract and retinal ganglion cell loss were not observed by BIO or histology.

BIO was used to examine the overall morphology of the eye after injection. The BIO images showed both the fundus and the gel inside the eye (Fig. 3). No retinal detachment, edema, or inflammation could be observed at all quadrants. The gel appeared transparent in the eye, and it moved slightly around the injection site. Although the gel was injected to the superior temporal region, we did not observe hydrogel sinking to the bottom as reported in other gel system.<sup>22</sup> For application in humans, the blocking of vision by the release depot is undesirable, and the transparent appearance and the relatively stable location of the gel in the eye may be a beneficial feature.

ERG measures the electrical responses of photoreceptors and the associated secondary neurons towards light stimulation. The light-adapted ERG (Fig. 4A)

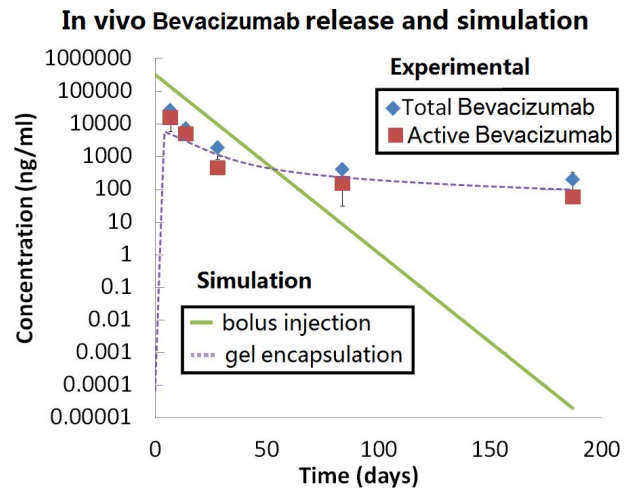


**Figure 7.** Comparing experimental measured Avastin (Roche Ltd) concentration in the vitreous after gel-formulation injection with simulated bolus injection and gel-formulation injection.

reflected the cone cell and cone cell related secondary neurons activity, while the dark-adapted ERG (Figs. 4B, 4C) reflected the combined responses generated from rod and cone cells, as well as their associated neurons. Our data show that the range of ERG fluctuation in eyes injected with gels were similar to the control, indicating there was no detectable change in retinal function after gel injection. The fluctuation of ERG measurement was similar to other reports.<sup>28,29</sup> The difference between the control group and gel injection groups at the same time points was not statistically significant either ( $P > 0.05$ ). Representative ERG profiles can be found in Supplementary Materials (Fig. S3).

To evaluate the potential changes at cellular level, histological analysis of the eye was conducted at the end point of the experiment. The result shows that the morphology of the cells, cell density, and thickness of different layers in the gel injection group were indifferent to the control group.

Taken together, these results suggest that the hydrogel is compatible to the rabbit eye after intravitreal injection.

The *in vivo* controlled release performance of the hydrogel formulation was evaluated by measuring the bevacizumab concentration in the vitreous at different time points. The experimental results were compared with simulations of both nonformulated bolus injection and the gel encapsulated formulation injection.

The bevacizumab pharmacokinetics in a normal rabbit eye after intravitreal injection has been measured and demonstrated to roughly follow the first order elimination kinetics model.<sup>13-15</sup> Using this

model, we constructed the intravitreal bevacizumab concentration profile over time after bolus injection of a 500- $\mu$ g dose, the same as the amount we used in the gel formulation. In contrast to the sharp decrease of intraocular bevacizumab concentration after bolus injection, the gel formulation helped to maintain a relatively stable drug concentration especially after 2 months. At the sixth month after injection, the concentration of bevacizumab was about 100 ng/mL (total: 193 ng/mL, active: 54 ng/mL), which was seven orders of magnitude higher than bolus injection ( $2 \times 10^{-5}$  ng/mL). Other published studies on bevacizumab controlled release formulations showed less significant improvement (e.g., five times higher than bolus injection).<sup>22,30</sup> According to the IC<sub>50</sub> of bevacizumab in vitro<sup>31</sup> and the concentration of VEGF in disease state in human eye,<sup>32</sup> the therapeutically relevant concentration should be in the order of 50 ng/mL. The formulation we tested was able to maintain the concentration above this level for at least 6 months.

Using classical compartment model and the in vitro release data (Supplementary Fig. S1), we simulated the concentration of bevacizumab in the rabbit eye after gel-formulated injection and compared it with the experimental result. The release rate from the depot was taken directly from the curve fitting of the in vitro release profile, while the elimination kinetics followed the well-established first order bevacizumab elimination in the rabbit vitreous. We found that the data generally fitted the simulation, confirming the effective gel formation in the eye in vivo. It should be noted that although the release rate was over predicted by the simulation for later time points (after 2 months), the simulated values at 3 and 6 months were still lower than the experimental measurements. This result indicates that the gel was likely to be degraded partially, which causes higher in vivo release than observed in the in vitro experiment. Because we chose HA as one of the main polymer component, the gel was likely to be degraded by hyalocyte, hyaluronidase, or other mechanisms in the vitreous.<sup>7-9</sup>

In our study, both the total and active bevacizumab was measured. For the total bevacizumab, a polyclonal rabbit anti-human IgG, which can bind to multiple epitopes of the bevacizumab, was used as the coating antigen in ELISA. To estimate the biologically active bevacizumab, ELISA plates were coated with VEGF, the target binding molecule for bevacizumab. We found that the active bevacizumab in the eye was always lower than the total bevacizumab, and

the ratio was kept at around 30% after 1 month (Supplementary Fig. S2). This result is consistent with a previous published study showing the degradative effect of vitreous on bevacizumab.<sup>33</sup>

## Conclusions

An in situ hydrogel-based ocular controlled delivery system for bevacizumab was evaluated in vivo. By simply mixing the two precursor polymers with the protein, the mixture can be injected to the eye as a solution and form a gel efficiently without either the addition of an initiator nor generating any by products. The system was found to be compatible to the rabbit eye and was able to maintain the bevacizumab in the vitreous at therapeutically relevant concentration for at least 6 months.

These results show that in situ chemically cross-linkable polymer-polymer hydrogels can be a potent delivery system for the controlled release of proteins in the eye.

## Acknowledgments

The authors thank Vincent W.H. Lee from the Hong Kong Eye Surgery Centre for the training of intraocular injection and the use of binocular indirect microscope.

Supported by the Hong Kong Research Grant Council (RGC), Innovation and Technology Fund (ITS/190/11), and the HKUST Bioengineering Graduate Program.

Disclosure: **Y. Yu**, None; **L.C.M. Lau**, None; **A.C.-Y. Lo**, None; **Y. Chau**, None

## References

1. Pieramici DJ, Rabena MD. Anti-VEGF therapy: comparison of current and future agents. *Eye (Lond)*. 2008;22:1330–1336. doi:10.1038/eye.2008.88.
2. Zhang K, Zhang L, Weinreb RN. Ophthalmic drug discovery: novel targets and mechanisms for retinal diseases and glaucoma. *Nat Rev Drug Discov*. 2012;11:541–559. doi:10.1038/nrd3745.
3. Genentech USA, Inc. Highlight of prescribing information for Lucentis. Available at: <http://>

- www.gene.com/download/pdf/lucentis\_prescribing.pdf. Accessed January 28, 2014.
4. Sampat KM, Garg SJ. Complications of intravitreal injections. *Curr Opin Ophthalmol*. 2010;21:178–183. doi:10.1097/ICU.0b013e328338679a.
  5. Yu Y, Chau Y. Formulation of in situ chemically-crosslinked hydrogel depots for protein release: from the blob model perspective. *Biomacromolecules*. 2014;16(1):56–65. doi:10.1021/bm501063n.
  6. Unterman SA, Marcus NA, Elisseff JH. Injectable polymers. In: Domb AJ, Kumar N, eds. *Biodegradable Polymers in Clinical Use and Clinical Development*. Wiley (Hoboken, NJ); 2011:632–655.
  7. Jacobson B. Degradation of glycosaminoglycans by extracts of calf vitreous hyalocytes. *Exp Eye Res*. 1984;39:373–385.
  8. Haddad A, Andre JC. Hyalocyte-like cells are more numerous in the posterior chamber than they are in the vitreous of the rabbit eye. *Exp Eye Res*. 1998;66:709–718.
  9. Schwartz DM, Shuster S, Jumper MD, Chang A, Stern R. Human vitreous hyaluronidase: isolation and characterization. *Curr Eye Res*. 1996;15:1156–1162.
  10. Balazs EA. Hyaluronan as an ophthalmic viscoelastic device. *Curr Pharm Biotechnol*. 2008;9:236–238.
  11. Yu Y, Chau Y. One-step “click” method for generating vinyl sulfone groups on hydroxyl-containing water-soluble polymers. *Biomacromolecules*. 2012;13:937–942. doi:10.1021/bm2014476.
  12. Suen W-LL, Chau Y. Size-dependent internalisation of folate-decorated nanoparticles via the pathways of clathrin and caveolae-mediated endocytosis in ARPE-19 cells. *J Pharm Pharmacol*. 2014;6:564–573. doi:10.1111/jphp.12134.
  13. Nomoto H, Shiraga F, Kuno N, et al. Pharmacokinetics of bevacizumab after topical, subconjunctival, and intravitreal administration in rabbits. *Invest Ophthalmol Vis Sci*. 2009;50:4807–4813. doi:10.1167/iovs.08-3148.
  14. Sinapis CI, Routsias JG, Sinapis AI, et al. Pharmacokinetics of intravitreal bevacizumab (Avastin®) in rabbits. *Clin Ophthalmol*. 2011;5:697–704. doi:10.2147/OPHTH.S19555.
  15. Bakri SJ, Snyder MR, Reid JM, Pulido JS, Singh RJ. Pharmacokinetics of intravitreal bevacizumab (Avastin). *Ophthalmology*. 2007;114:855–859. doi:10.1016/j.ophtha.2007.01.017.
  16. Miyake T, Sawada O, Kakinoki M, et al. Pharmacokinetics of bevacizumab and its effect on vascular endothelial growth factor after intravitreal injection of bevacizumab in macaque eyes. *Invest Ophthalmol Vis Sci*. 2010;51:1606–1608. doi:10.1167/iovs.09-4140.
  17. Schwartz SG, Scott IU, Flynn HW, Stewart MW. Drug delivery techniques for treating age-related macular degeneration. *Expert Opin Drug Deliv*. 2014;11:61–68. doi:10.1517/17425247.2013.859135.
  18. Derwent J, Mieler W. Thermoresponsive hydrogels as a new ocular drug delivery platform to the posterior segment of the eye. *Trans Am Ophthalmol Soc*. 2008;106:206–214.
  19. Park D, Shah V, Rauck BM, Friberg TR, Wang Y. An anti-angiogenic reverse thermal gel as a drug-delivery system for age-related wet macular degeneration. *Macromol Biosci*. 2013;13:464–469. doi:10.1002/mabi.201200384.
  20. Xu X, Weng Y, Xu L, Chen H. Sustained release of Avastin® from polysaccharides cross-linked hydrogels for ocular drug delivery. *Int J Biol Macromol*. 2013;60(Complete):272–276.
  21. Wang C-H, Hwang Y-S, Chiang P-R, Shen C-R, Hong W-H, Hsiue G-H. Extended release of bevacizumab by thermosensitive biodegradable and biocompatible hydrogel. *Biomacromolecules*. 2012;13:40–48. doi:10.1021/bm2009558.
  22. Rauck BM, Friberg TR, Medina CA, et al. Biocompatible reverse thermal gel sustains the release of intravitreal bevacizumab in vivo. *Invest Ophthalmol Vis Sci*. 2014;55:469–476. doi:10.1167/iovs.13-13120.
  23. Hwang Y-S, Chiang P-R, Hong W-H, et al. Study in vivo intraocular biocompatibility of in situ gelation hydrogels: poly(2-ethyl oxazoline)-block-poly(ε-caprolactone)-block-poly(2-ethyl oxazoline) copolymer, matrigel and pluronic F127. *PLoS One*. 2013;8:e67495. doi:10.1371/journal.pone.0067495.
  24. Wang W. Instability, stabilization, and formulation of liquid protein pharmaceuticals. *Int J Pharm*. 1999;185:129–188.
  25. Tyagi P, Barros M, Stansbury JW, Kompella UB. Light-activated, in situ forming gel for sustained suprachoroidal delivery of bevacizumab. *Mol Pharm*. 2013;10:2858–2867. doi:10.1021/mp300716t.
  26. Jha AK, Xu X, Duncan RL, Jia X. Controlling the adhesion and differentiation of mesenchymal stem cells using hyaluronic acid-based, doubly crosslinked networks. *Biomaterials*. 2011;32:2466–2478. doi:10.1016/j.biomaterials.2010.12.024.

27. Lévesque SG, Shoichet MS. Synthesis of cell-adhesive dextran hydrogels and macroporous scaffolds. *Biomaterials*. 2006;27:5277–5285. doi:10.1016/j.biomaterials.2006.06.004.
28. Schramm C, Spitzer MS, Henke-Fahle S, et al. The cross-linked biopolymer hyaluronic acid as an artificial vitreous substitute. *Invest Ophthalmol Vis Sci*. 2012;53:613–621. doi:10.1167/iovs.11-7322.
29. Lawwill T. Practical rabbit electroretinography. *Am J Ophthalmol*. 1972;74:135–141.
30. Mordenti J, Thomsen K, Licko V, et al. Intraocular pharmacokinetics and safety of a humanized monoclonal antibody in rabbits after intravitreal administration of a solution or a PLGA microsphere formulation. *Toxicol Sci*. 1999;52:101–106.
31. Wang Y, Fei D, Vanderlaan M, Song A. Biological activity of bevacizumab, a humanized anti-VEGF antibody in vitro. *Angiogenesis*. 2004;7:335–345. doi:10.1007/s10456-004-8272-2.
32. Praidou A, Papakonstantinou E, Androudi S, Georgiadis N, Karakiulakis G, Dimitrakos S. Vitreous and serum levels of vascular endothelial growth factor and platelet-derived growth factor and their correlation in patients with non-proliferative diabetic retinopathy and clinically significant macula oedema. *Acta Ophthalmol*. 2011;89:248–254. doi:10.1111/j.1755-3768.2009.01661.x.
33. Liu DT-L, Xu L, Pang C-P, Lam DS-C, Yam GH-F. Disruption of bevacizumab (Avastin) activity by vitreous matrix gel. *J Clin Exp Ophthalmol*. 2011;2:140.